AFRL-RX-WP-JA-2015-0079

DEVELOPMENT OF A TEST TO EVALUATE AEROTHERMAL RESPONSE OF MATERIALS TO HYPERSONIC FLOW USING A SCRAMJET WIND TUNNEL (POSTPRINT)

George Jefferson and Michael K. Cinibulk
AFRL/RXCC

Triplicane A. Parthasarathy and M. Dennis Petry
UES, Inc.

Tarun Mathur
ISSI

Mark R. Gruber
AFRL/RZAS

MAY 2010
Interim Report

AIR FORCE RESEARCH LABORATORY
MATERIALS AND MANUFACTURING DIRECTORATE
WRIGHT-PATTERSON AIR FORCE BASE OH 45433-7750
AIR FORCE MATERIEL COMMAND
UNITED STATES AIR FORCE

NOTICE AND SIGNATURE PAGE

Using Government drawings, specifications, or other data included in this document for any purpose other than Government procurement does not in any way obligate the U.S. Government. The fact that the Government formulated or supplied the drawings, specifications, or other data does not license the holder or any other person or corporation; or convey any rights or permission to manufacture, use, or sell any patented invention that may relate to them.

Qualified requestors may obtain copies of this report from the Defense Technical Information Center (DTIC) (http://www.dtic.mil).

AFRL-RX-WP-JA-2015-0079 HAS BEEN REVIEWED AND IS APPROVED FOR PUBLICATION IN ACCORDANCE WITH ASSIGNED DISTRIBUTION STATEMENT.

//Signature//

PATRICK S. CARLIN, Project Engineer
Composite Materials and Processing Section
Composite Branch
Structural Materials Division

//Signature//

SEAN C. COGHLAN, Chief
Composite Materials and Processing Section
Composite Branch
Structural Materials Division

//Signature//

ROBERT T. MARSHALL, Deputy Chief
Structural Materials Division
Materials And Manufacturing Directorate

This report is published in the interest of scientific and technical information exchange and its publication does not constitute the Government's approval or disapproval of its ideas or findings.

REPORT DOCUMENTATION PAGE

Form Approved
OMB No. 0704-0188

1. REPORT DATE *(DD-MM-YY)*	2. REPORT TYPE	3. DATES COVERED *(From - To)*
May 2010	Interim	06 April 2010 – 07 April 2010

4. TITLE AND SUBTITLE
DEVELOPMENT OF A TEST TO EVALUATE AEROTHERMAL RESPONSE OF MATERIALS TO HYPERSONIC FLOW USING A SCRAMJET WIND TUNNEL (POSTPRINT)

5a. CONTRACT NUMBER
FA8650-10-D-5226-0002

5b. GRANT NUMBER

5c. PROGRAM ELEMENT NUMBER
62102F

6. AUTHOR(S)
See back

5d. PROJECT NUMBER
4347

5e. TASK NUMBER

5f. WORK UNIT NUMBER
X0L5

7. PERFORMING ORGANIZATION NAME(S) AND ADDRESS(ES)
See back

8. PERFORMING ORGANIZATION REPORT NUMBER

9. SPONSORING/MONITORING AGENCY NAME(S) AND ADDRESS(ES)
Air Force Research Laboratory
Materials and Manufacturing Directorate
Wright-Patterson Air Force Base, OH 45433-7750
Air Force Materiel Command
United States Air Force

10. SPONSORING/MONITORING AGENCY ACRONYM(S)
AFRL/RXCCM

11. SPONSORING/MONITORING AGENCY REPORT NUMBER(S)
AFRL-RX-WP-JA-2015-0079

12. DISTRIBUTION/AVAILABILITY STATEMENT
Distribution Statement A. Approved for public release; distribution unlimited.

13. SUPPLEMENTARY NOTES
Journal article published in *Int. J. Appl. Ceram. Technol., 8 [4] 832–847 (2011).* ©2010 The American Ceramic Society. The U.S. Government is joint author of the work and has the right to use, modify, reproduce, release, perform, display or disclose the work. Document contains color. The final publication is available at http://onlinelibrary.wiley.com/doi/10.1111/j.1744-7402.2010.02515.x/abstract

14. ABSTRACT
A methodology to evaluate the aerothermal response of sharp leading edge materials by exposing them directly to hypersonic flow up to Mach 7 was developed and evaluated. The exposure was conducted using a prototype scramjet engine as a wind tunnel. A sample holder was designed using combustion fluid dynamics results as inputs into structural models. The rig conditions were evaluated and found to be close to those during free flight, with respect to aerothermal parameters of importance for material survivability. Samples of ultra high-temperature ceramics and SiC were found to withstand the short-term exposure that simulated Mach 6.5 at 25 km altitude.

15. SUBJECT TERMS
leading edge, UHTC, SiC, hypersonic, scramjet engine

16. SECURITY CLASSIFICATION OF:			17. LIMITATION OF ABSTRACT:	18. NUMBER OF PAGES	19a. NAME OF RESPONSIBLE PERSON (Monitor)
a. REPORT	b. ABSTRACT	c. THIS PAGE			Patrick S. Carlin
Unclassified	Unclassified	Unclassified	SAR	20	19b. TELEPHONE NUMBER *(Include Area Code)* (937) 904-5547

REPORT DOCUMENTATION PAGE Cont'd

6. AUTHOR(S)

George Jefferson and Michael K. Cinibulk - AFRL/RXLN

Triplicane A. Parthasarathy and M. Dennis Petry - UES, Inc.

Tarun Mathur – ISSI

Mark R. Gruber - AFRL/RZAS

7. PERFORMING ORGANIZATION NAME(S) AND ADDRESS(ES)

AFRL/RXLN
2941 Hobson Way
Bldg 654, Rm 136
Wright-Patterson AFB OH 45433

UES Inc.
4401 Dayton-Xenia Rd.
Dayton, OH 45432-1894

ISSI
Dayton, Ohio 45432

AFRL/RZAS
Wright-Patterson AFB, Ohio 45433

Int. J. Appl. Ceram. Technol., 8 [4] 832–847 (2011)
DOI:10.1111/j.1744-7402.2010.02515.x

International Journal of
Applied Ceramic TECHNOLOGY
Ceramic Product Development and Commercialization

Development of a Test to Evaluate Aerothermal Response of Materials to Hypersonic Flow Using a Scramjet Wind Tunnel

Triplicane A. Parthasarathy,[*,†] M. Dennis Petry,[†] George Jefferson, and Michael K. Cinibulk

Air Force Research Laboratory, Materials and Manufacturing Directorate, AFRL/RXLN, Wright-Patterson AFB, OH 45433

Tarun Mathur

ISSI, Dayton, Ohio 45432

Mark R. Gruber

Air Force Research Laboratory, Propulsion and Power Directorate, AFRL/RZAS, Wright-Patterson AFB, Ohio 45433

A methodology to evaluate the aerothermal response of sharp leading edge materials by exposing them directly to hypersonic flow up to Mach 7 was developed and evaluated. The exposure was conducted using a prototype scramjet engine as a wind tunnel. A sample holder was designed using combustion fluid dynamics results as inputs into structural models. The rig conditions were evaluated and found to be close to those during free flight, with respect to aerothermal parameters of importance for material survivability. Samples of ultra high-temperature ceramics and SiC were found to withstand the short-term exposure that simulated Mach 6.5 at 25 km altitude.

This work was financially supported under USAF Contract # FA8650-04-D-5233.
[*]triplicane.parthasarathy@wpafb.af.mil
[†]UES, Inc., Dayton OH 45432

Introduction

The interest in easy access to space and global reach within as little as 2 h has resulted in renewed interest in hypersonic flights, which use a reuseable air breathing vehicle that can travel at or greater than Mach 8.[1] Recent short-term flight tests by NASA (X43a) have shown that the concept of a scramjet engine works at speeds of Mach 7 and 10.[2,3] Despite these successes, the realization of such a vehicle in reusable form, will require novel materials that can handle the aerothermal conditions imposed on some of the critical parts.[4] The inlet cowl leading edge (LE) of the engine is one of the critical components and it is anticipated that the material temperature could reach as high as 2000°C through aerothermal heating at Mach 8.[5] This in turn has spurred research and development of ultra-high-temperature ceramics (UHTC), which show promise for such applications.[6] These materials are being evaluated using several different laboratory tests by different investigators, ranging from isothermal anneals in an air furnace to expensive arc-jet testing.[6] While arc-jet testing is considered the most stringent, none of the tests used to date are known to completely simulate the actual conditions that the material will experience in use. A list of the test methods used to date are shown in Table I, along with the relative merits and demerits of the tests in relation to how well they simulate actual conditions during hypersonic flight, as discussed briefly below.

The conditions experienced by a sharp body under hypersonic flow conditions have been the subject of modeling since early 1950s.[7–9] These models show clearly that a material experiences a unique combination of thermal and environmental effects under hypersonic flow conditions. Key parameters that represent these conditions with respect to material survivability are heat flux, total or stagnation temperature, total or stagnation pressure, dynamic pressure, fluid velocity at the material surface, fluid composition, degree of dissociation of gaseous elements, and catalytic recombination at the material's surface. In addition, under realistic conditions, resistance to vibrations and thermal shock will also be important. Most of the experiments are conducted in a laboratory furnace, thus assigning the total temperature as the key parameter of interest by default; all other factors are ignored. The tests that use laser as a heat source (e.g., LHMEL) focus on reproducing the appropriate heat flux, and in some cases include fluid flow. The hypersonic wind tunnels focus on the free stream fluid velocity. The plasmatron or arc-jet test, generally considered to be the closest to real conditions, focuses on reproducing the heat flux and includes the effect of catalytic recombination of gases. Finally, testing using real hypersonic flights is rare and expensive.[2]

In this work, a new method of evaluating materials under hypersonic flow conditions was developed and evaluated. A direct-connect scramjet combustor rig, designed based on the needs for hypersonic flight and described elsewhere,[10] was explored for use as a wind tunnel. A methodology to introduce samples into the flow path of the combustor was examined using a combination of modeling and experimental trials. In the final design that emerged after several iterations, a LE configuration was used to expose two samples, one of SiC and another of 20% vol SiC–HfB_2. Both samples were tested successfully using this novel method under conditions that we show represent free stream flight Mach number of 6.5 at an altitude of 25 km. Instrumentation of the samples was used to validate aerothermal models. The test was examined critically in terms of its ability to subject the sample to aerothermal conditions that match the conditions predicted to exist in real flight. Results show that conditions very close to real flight can be reproduced quite well with respect to heat flux, total temperature, and fluid velocity, and reasonably well with respect to fluid composition. The rig also included realistic mechanical and thermo-mechanical loading in terms of vibrations and thermal shock.

This paper is organized as follows. We start with a brief description of the rig, and present the modeling methods that helped in preliminary designs, before presenting the sample holder design and the actual exposure experiments performed. After presenting the results of the model and experiments, we end with a discussion of how well the test simulates free flight conditions.

Scramjet Direct-Connect Rig

Gruber *et al.*[10] have designed and fabricated a direct-connect full-scale scramjet combustor test facility for studies on supersonic combustion, fuel injection, flame holding, and other aspects of propulsion. This test facility provides combustor inlet flow conditions corresponding to flight Mach numbers between 3.5 and 7, at dynamic pressures up to 95.8 kPa. Most of the major

Table I. A List of Various Test Methods Used to Simulate Material Effects During Hypersonic Flight Conditions, Along with their Relative Merits and Demerits

Method	Imposed condition	Merits	Demerits
Air furnace	$T_{tot.}$ (or calc. $T_{mat.}$)	Ease of use	Ignores flow (shear) No thermal gradient/transients Does not include catalytic recombination Ignores mechanical effects
Laser (LHMEL)	Calculated heat flux	High temperature, heating rates	Ignores emissivity changes No catalytic recombination effects Low fluid velocities, if present Typically uses flat substrate geometry Ignores mechanical effects
Hypersonic wind tunnel	Hypersonic fluid flow	Very high fluid velocities	Imposes low T_{tot} Wrong gas chemistry
Plasmatron (arc jet)	Calculated heat flux	Catalytic recombination	Expensive, imposes low flow Uses mostly dissociated gases Ignores mechanical effects
Real hypersonic flights	Real conditions	Real conditions	Rare, expensive
Scramjet wind tunnel (present work)	Hypersonic combustion	Includes all effects	Inaccuracies in gas chemistry Possible inaccuracy in degree of dissociation above Mach 7

calc., calculated; tot., total; mat., material.

components of the new facility are water cooled. The facility includes a variety of conventional and advanced instrumentation for accurate documentation of combustor inlet and exit conditions. The rig has been calibrated to obtain profiles of pitot pressure, total temperature, and wall static pressure distributions for a wide range of inlet conditions. In addition, combustion fluid dynamics (CFD) modeling of the rig has been conducted to obtain predicted conditions within the rig, and found to be in good agreement with experiments. Further details can be found elsewhere.[10–13]

In a more recent development, the rig has been redesigned to an axisymmetric configuration and similar calibration and CFD modeling have been completed, results of which are not yet published, but were used in interpreting the results of this work. The axisymmetric rig was calibrated the same way as the rectangular rig, and the entire operation was identical from the perspective of the user. Preliminary studies in this work where model development, sample holder design, and validation were conducted used the first-generation rig of a rectangular cross section, while later runs that included the successful exposure of samples to near-flight conditions were conducted using the next-generation rig with an axisymmetric cross section.

Modeling Fluid-Structure Interactions Under Hypersonic Flow

The objective of the modeling work was to simultaneously (a) develop and validate a hypersonic flow fluid-structure interaction model and (b) use the model to help to design a sample holder to be used for exposing samples of LE prototype subcomponents. The modeling involved a combination of CFD and FEA models

along with equations describing aerothermal effects of hypersonic flow. For a given operating condition of the rig, the relevant fluid parameters (detailed below) obtained from CFD were used to calculate the heat flux distribution on the material using aerothermal models. With this heat flux distribution as input, an FEA model was used to calculate thermal and mechanical states of the sample holder as a function of the material choice and geometry. Using different geometry and material parameters, and validating predictions using preliminary experiments, a suitable design was evolved. Details of the LE sample geometry and position in the rig are described later; briefly, the sample is to have a sharp radius of curvature and located beyond 0.5 in. from the combustor wall to avoid boundary layer effects.

CFD simulations of the unobstructed rig were performed using the CFD++ code, a general-purpose CFD tool developed by Metacomp Technologies (Agoura Hills, CA). CFD++ has several types of Riemann solvers; the HLLC Riemann solver with Minmod flux limiting was used in the simulations used here. At solid surfaces, an advanced two-layer wall function with the blended mode of equilibrium and nonequilibrium was used to reduce grid requirements. The turbulent Schmidt and Prandtl numbers that control the modeled turbulent transport of mass and energy, respectively, were set to constant values. For runs with combustion, ignition was achieved through the use of a quasi-global ethylene reaction model and by reducing the activation energy by an order of magnitude.

The CFD results for the static temperature, pressure, and fluid velocities over the region of interest in the rig are shown in Fig. 1 for the case of full combustion with an equivalence ratio (ER) of 0.5, along with the total temperature contours calculated using the well-known compressible flow equations[7]:

$$M = U/\sqrt{\gamma(R/M_w)T} \tag{1}$$

$$T_t = T_1\left(1 + \frac{\gamma - 1}{2}M^2\right) \tag{2}$$

where U is the fluid velocity, R the universal gas constant, M_w the molecular weight of air, T_1, T_t the static, and total/stagnation temperatures, respectively, M the mach number, and γ the ratio of specific heats of air.

These results were used in an FEM structural model to predict thermal gradients and stresses resulting from the same. The fluid heat flux was modeled using aerothermal equations as given in the report by Ames Research Staff[7] and the aerothermal heat flux equation is given by Zoby[14] as

$$Q_w\,(\mathrm{W/m^2}) = 3.88 \times 10^{-4}\sqrt{\frac{p_{t2}\,(\mathrm{Pa})}{r\,(\mathrm{m})}}(h_{aw} - h_w) \tag{3}$$

$$(h_{aw} - h_w)\,(\mathrm{kJ/kg}) = C_p(T_t - T_{wall}) \tag{4}$$

where Q_w is the stagnation heat flux on the material, r the radius of curvature of the cylindrical sample, h_{aw} the adiabatic wall enthalpy, h_w the enthalpy of air calculated at the material wall temperature, C_p the specific heat of air, the T_{wall} the material wall temperature. The stagnation or total pressure behind the bow shock, p_{t2}, is given by the Raleigh pitot tube formula:

$$p_{t2} = p_1\left(\frac{\gamma+1}{2}\right)^{\frac{\gamma}{\gamma-1}}\left(\frac{(\gamma+1)M^2}{2\gamma M^2 - (\gamma-1)}\right)^{\frac{1}{\gamma-1}} M^2 \tag{5}$$

where p_1 is the free stream (static) pressure. The quantities p_{t2} and T_t were taken from the CFD results as dependent on the distance from the containment wall, and the distribution over the cylindrical edge was assumed to follow a cosine distribution, that is $Q(\theta) = Q_{cw}(1 - T_{wall}/T_t)\cos\theta$, where Q_{cw} is the cold wall flux found by setting $T_{wall} = 0$ in Eq. (3) and θ is the angle measured from the stagnation point. The flux is taken to drop off as the square root of distance over the flat portion of a wedge-shaped specimen.[5]

Radiation exchange between the sample and the containment vessel is important to incorporate into the model. The radiative heat flux was calculated using the measured containment wall (sink) temperature of 280°C. The metal plate holding the sample holder was fixed around its outer edge to a temperature graded from 150°C inside the rig (measured using thermocouple) to 40°C (estimate) outside. The calculations included a gap conductance condition between the holder and the plate. Both steady-state temperatures with full combustion on and the transients during cool down were modeled, along with stresses arising from the same. The calculations were performed for two candidate materials, alumina and SiC, which were also tested experimentally. The results were compared with experimental measurements of temperature of the sample holder, discussed in the next section.

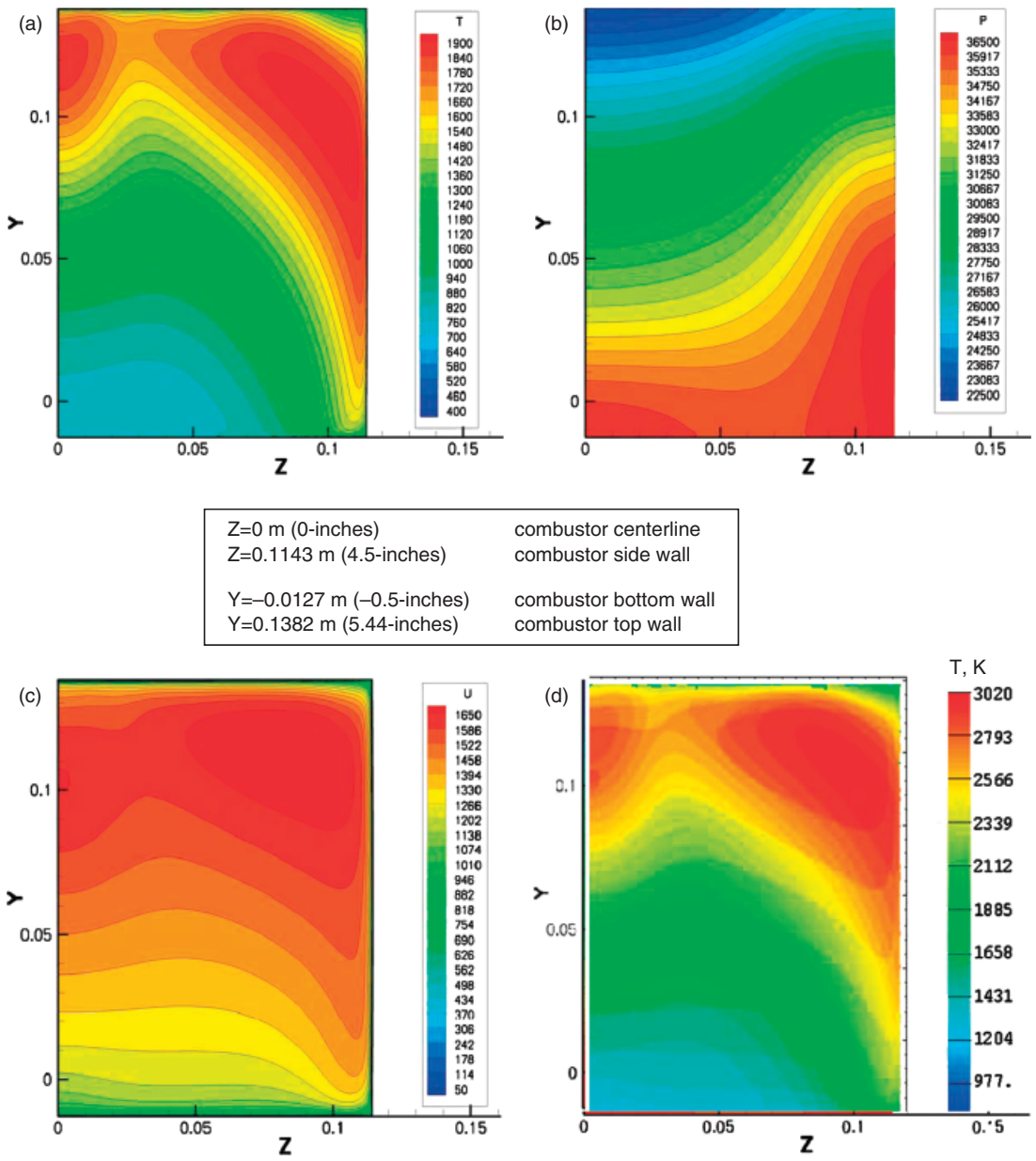

Fig. 1. Results from combustion fluid dynamics calculations of (a) static temperature in K (b) static pressure in Pa (c) fluid velocity in m/s, and (d) calculated total temperature across the combustor section where the samples were designed to be introduced. The dimensions are in meters. The calculations were for an equivalence ratio of 0.5.

Sample Holder Designs

Requirements that the sample holder design had to meet included that (a) it can sustain the mechanical and thermal loading of the scramjet flow path conditions, (b) it can hold a LE sample in the flow path, and (c) it allows for instrumented measurement of temperature of the sample without an obstruction to the flow. The current propulsion design requirements call for the cowl LE of the hypersonic engine to have a 762 μm (30 mil)

radius of curvature at the end facing the flow, with its thickness increasing with distance, away from the flow at a wedge angle of 12°. Aerothermal modeling conducted in an earlier study has shown that there is a steep gradient in heat flux at the LE and that the material temperature will drop drastically away from the edge at a rate of over a several hundred degrees C/mm.[5] Thus, it was determined for the purposes of this work that a LE that is 12.7 mm (0.5 in.) long was sufficient to reproduce the high temperatures at the tip and the steep temperature gradient that the material will have to withstand during service. The limitations of space in the flow path determined the span length of the sample. A 12.7 mm (0.5 in.)-long sample was considered appropriate such that two samples could be introduced during a single run (Fig. 2). The heat-flux-induced thermal gradients during steady state and the thermal shock resulting from abrupt cooling were the most stringent conditions that imposed the highest stresses in the material. These conditions were used to evaluate material survivability. The intensity and spectra of the mechanical vibrations were unknown *a priori* and had to be studied through actual trials.

A schematic of the basic sample holder design concept is shown in Fig. 2. After a few iterations, a dovetail

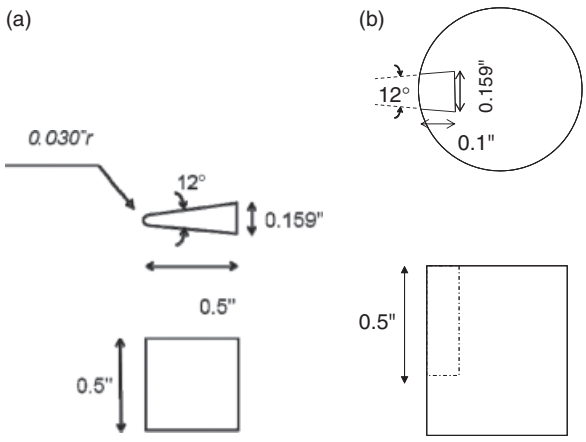

Fig. 2. Basic aspects of the design of (a) the sample and (b) the sample holder. The sample was required to have a leading edge radius of curvature of 762 μm (30 mils) and a wedge angle of 12° as per propulsion performance-based design. The sample length and width were determined based on available flow path dimensions in the scramjet rig. The sample holder was designed to have a dovetail with a close fit tolerance to prevent vibrational chatter. The fit was adjusted in some cases with ceramic fiber tows between the sample and the base of the groove.

holder was selected, because it eliminates any further machining of the sample and reduces the possibility of flaw-induced premature failure. In terms of material choice and attachment to the combustor wall, two designs were considered, a hot uncooled ceramic holder and a water-cooled metallic holder. The uncooled ceramic holder was considered as it provides the least intrusion to the thermal environment, while the cooled metallic holder was considered because set screws could be used to firmly hold the LE samples and because it was expected to be much more reliable and reusable. Further, the metallic holder could be made longer and thus was useful to test multiple LE specimens in a single run.

The first design based on an uncooled ceramic holder was used for model validation, in which the sample holder without the LE sample and the dovetail groove was run to obtain thermal profiles. Evaluation of the stability of the holder and thermal response of the material were conducted using alumina and SiC as material choices. A schematic of the geometry and other details used in this evaluation run is shown in Fig. 3. The ceramic holder along with the base plate was held in place through a window opening in the combustor, to which the metallic base was mechanically attached. The ceramic holder was held in place as shown in Fig. 3. A thermocouple was attached to the holder through a blind hole from the backside, such that the material temperature within 2.5 mm of the front LE could be measured and compared with model predictions.

Based on the results of the above-mentioned trials, the setup shown in Figs. 4a and b was designed, fabricated, and tested in the scramjet direct connect rig using LE samples made of SiC and 20% vol SiC–HfB_2. The ceramic holder shown in Fig. 4a had the same thermocouple design as used in the preliminary runs and relied on friction in the dovetail joint to retain the sample.

The metal holder shown in Fig. 4b was an internally water-cooled Inconel tube with a protective coating on the hot side. The hot side (front face) of the tube was protected with a plasma-sprayed zirconia thermal barrier coating (TBC). This metallic holder used set screws to prevent the possible slip of the sample within the dovetail. The dovetail holder was made of inconel and was attached to the tube by TIG welding. Monitoring the temperature of the LE samples at the back side was accomplished through an insertion of a thermocouple through a small diameter tube that ran across the diameter of the sample holder tube as shown in Fig. 4b.

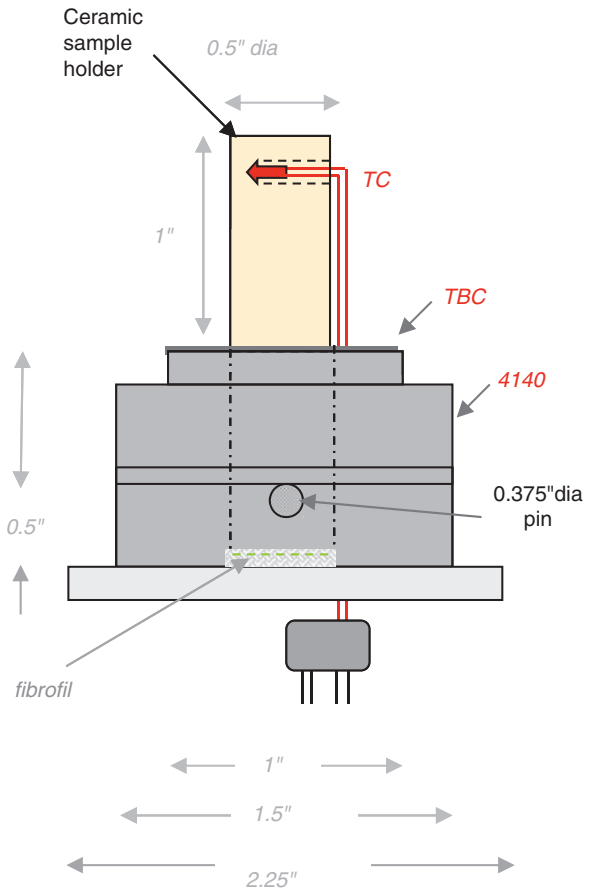

Fig. 3. Schematic drawing of the first sample holder design that was used to validate the aerothermal model. The shaded regions represent 4140 steel, which sat in an existing window boss in the combustor wall that was water cooled. The cream region is the leading edge sample holder, which was made of either alumina or SiC, the two materials chosen for the trial runs. The thermocouple was at a location of 2.5 mm from the leading edge of the cylindrical sample holder, which was exposed to hypersonic flow. The pin was used to locate the sample holder in the proper orientation, and the fibrofil was used to dampen vibrations.

Experiments

The details of the scramjet operations and the conditions of operations can be found in Gruber and colleagues.[10–13] The conditions in the chamber behind the combustor, in which the samples were exposed, were derived from prior calibrations carried out on the rig, described in Gruber and colleagues.[10–13] In the present work, the sample holders with or without the LE samples were introduced through a preexisting window opening (instrumentation port) in the rig in the post-combustion exhaust section. The rig was operated under two settings, one using only vitiated air and another with combustion. In the vitiated air condition, heat is added through the controlled combustion of compressed natural gas, but the loss of oxygen through combustion is compensated by the addition of the appropriate amount of oxygen. Thus, in the vitiated condition, the oxygen partial pressure of the gas is very close to ambient air, while the combustion condition introduced a further change in chemistry where oxygen upon reaction with the fuel is replaced with carbon dioxide and water. The gas chemistry changes with the ER, which is the ratio of fuel to air. The ER affects the gas chemistry along with enthalpy of the flowing gas arising from combustion. The ER was variable during the test and was gradually increased until the desired material temperature was reached or the specimen failed. The temperature readings were continually monitored, and in all but one experiment the specimens were continually monitored through a window using a standard optical video camera. The rig is instrumented to continually monitor the parameters of the run; these parameters along with prior calibration yielded the static pressure, total temperature, and fluid velocity at the location of the specimens. These parameters were used to interpret the conditions to which the sample or sample holder were subjected. The combustor was typically started using a vacuum pulled from the exhaust side, before compressed air was introduced from the inlet side. The vitiator was started next and the temperature of the fluid slowly increased in fixed calibrated increments denoted by total temperature settings. Finally, the combustor was turned on at a fixed ER value, typically 0.3, before being increased to a predetermined final ER value. The run segments with full combustion were limited in duration to prevent the temperature of the combustor walls from exceeding their limits. A typical combustion segment was run for 30 s at a given ER value, before the water-cooled combustor walls would get too hot to continue, at which time the combustor would be shut down to the vitiator state, for a few minutes before another combustor run could commence.

Initial runs were designed to examine the durability of the sample holder and to compare material temperatures with model predictions. All of these runs were made using the rectangular cross-section configuration of the scramjet rig described by Gruber *et al.*[10]

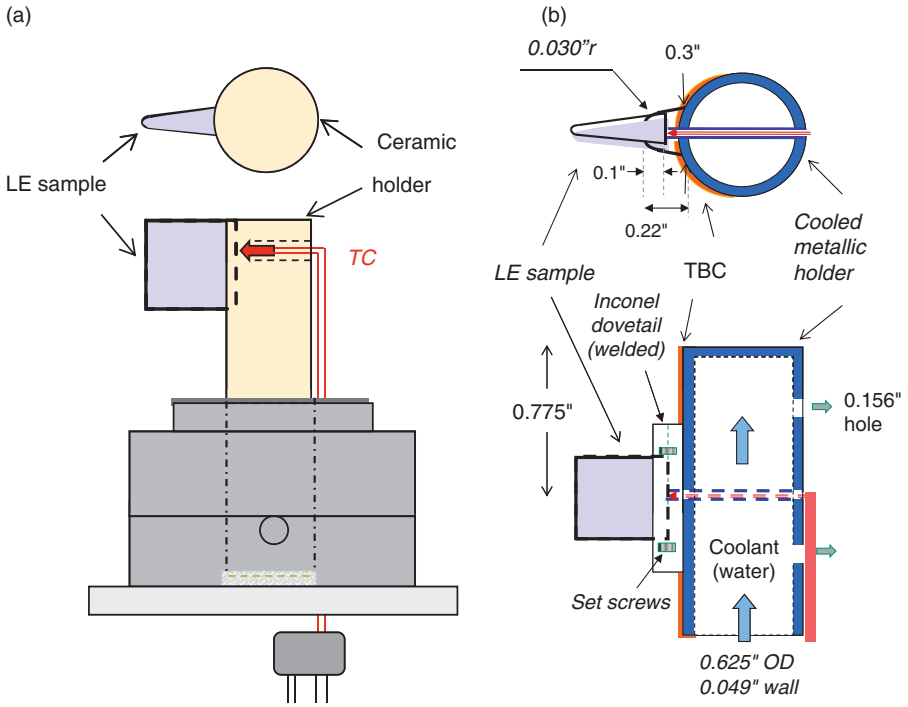

Fig. 4. Schematic sketches of the two designs for holding and exposing leading edge samples in the flow path of the scramjet direct connect rig. In (a), the sample holder is uncooled ceramic with minimal intrusion to thermal exposure, and in (b), the sample is held firmly in place using set screws in a water-cooled metallic holder, which offers a more robust and reusable design.

Alumina was selected as the material for the first test of the ceramic holder, based on availability and cost. The experimental setup had provisions to expose two samples in a given run, one sample being close to the center of the rig and the other away from the center. The alumina holder survived the vitiator only-setting, and survived the combustor runs for ER settings up to 0.5; but it failed under thermal shock during combustor shut down. The second material choice for the ceramic holder was SiC, and this material withstood several segment runs of the combustor for ER settings of 0.6, 0.7, 0.8, and 0.9 with associated total temperatures of approximately 2200, 2250, 2350, and 2400 K, respectively. The temperatures at the location shown in Fig. 3 were measured continuously for all these runs. Based on this, LE samples were run with the SiC sample holder in the configuration shown in Fig. 4a. Unfortunately, the samples did not stay in the holder during this run.

The water-cooled inconel tube sample holder was used for the remaining runs as it provided for a means of retaining the LE samples through the use of set screws as shown in Fig. 4b. This sample holder was inserted into the scramjet rig with an axisymmetric cross section. Two LE samples, one made of SiC and one made of 20% vol SiC–HfB_2 were run using this metallic holder in the axisymmetric rig. Both samples survived several segments of full combustor runs for ER values of 0.3, 0.4, and 0.45, which corresponded to total temperatures of 1600, 1800, and 1900 K, respectively. These runs confirmed that a means to subject LE samples to hypersonic flow was achieved.

Results

The results obtained from the modeling work and the experimental work will be presented together in this section for the sake of clarity. The model results for the sample holder will be presented first along with experimental data demonstrating validation of the model. The model simulations with the LE samples in the holder will be presented next, along with the experimental results for the runs with LE samples.

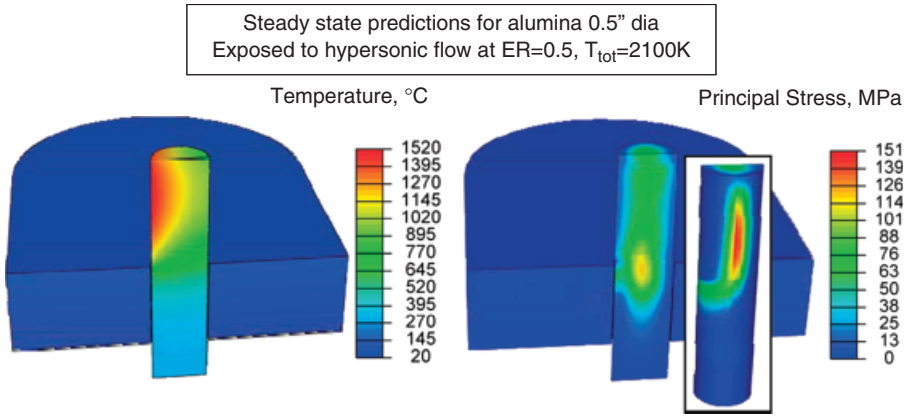

Fig. 5. Predictions of the model under steady state for the case of alumina, 12.7 mm (0.5 in.) in diameter exposed to hypersonic flow inside the scramjet rig for the case of vitiator+combustor at equivalence ratio (ER) = 0.5, which corresponds to a total temperature of 2100 K. The peak temperature at the leading edge is predicted to be 1780 K, with a gradient-induced stress of 151 MPa. For SiC, the peak temperature was predicted to be 1400 K with a gradient-induced stress < 10 MPa.

Figure 5 shows the temperature and stresses calculated for the alumina sample holder at steady state for the case of full combustion with ~2100 K total temperature, obtained for a ER setting of 0.5. It is observed that the alumina surface temperature is predicted to reach a maximum at the LE, up to a value of 1780 K (1507°C), which is within the allowable range for alumina. The thermal-gradient-induced stress is rather high, 151 MPa, but is within the typical fracture strength of alumina, and within the creep limits for

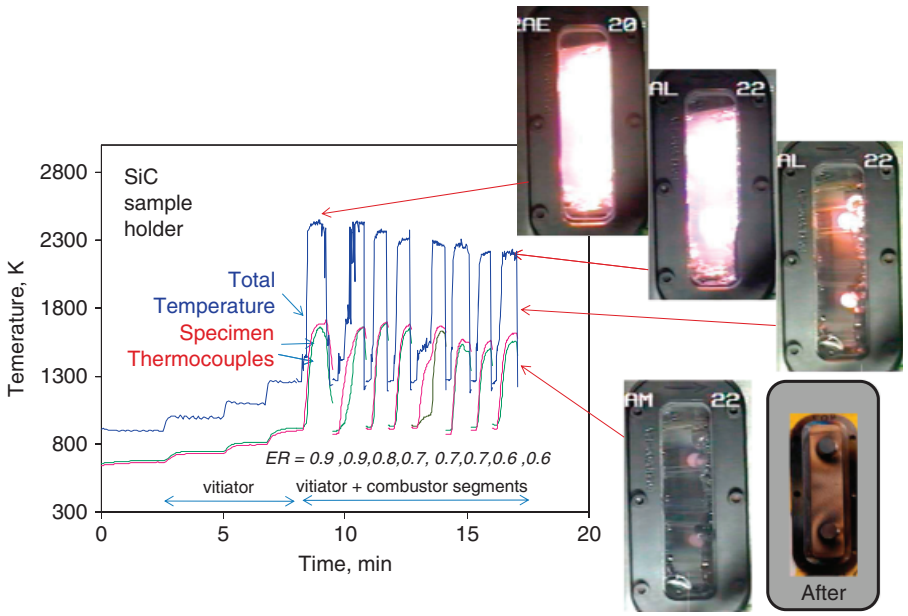

Fig. 6. The total temperatures (from calibration) and specimen thermocouple readings measured during a run on the scramjet rig, with two SiC sample holders placed in the flowpath. The equivalence ratio (ER) settings, ER values, are given for each combustor segment. Snapshots from the movie taken during the run are included for two ER cases as well as during combustor shutdown. The last image shows the intact SiC sample holders after the eight combustor segments.

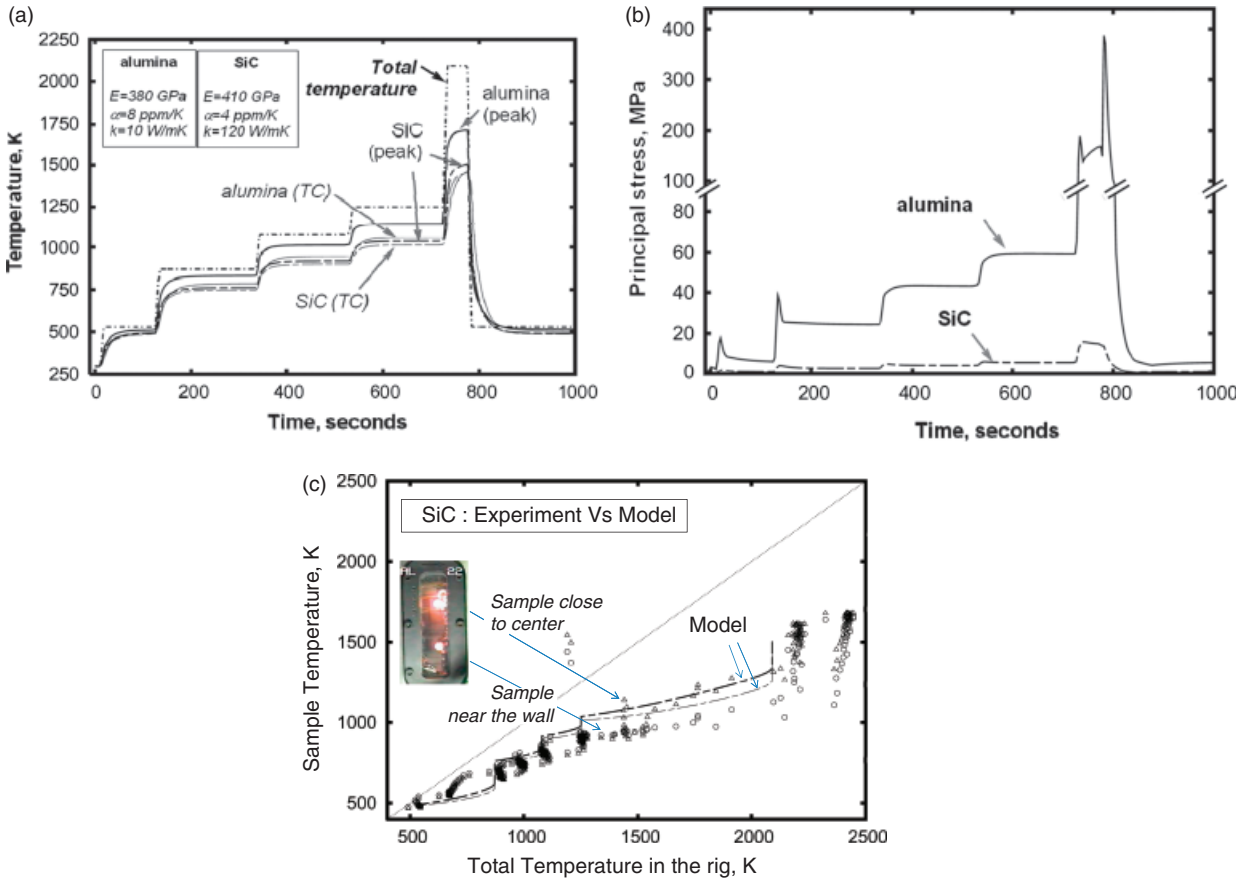

Fig. 7. (a) Model predictions for the sample temperatures at the surface (peak) and at the TC location (2.5 mm from surface) for alumina and SiC are shown as a function of time along with the total temperature of the gases. In (b), the principal stresses predicted by the model are shown as a function of time, including those during the shut-down transients for alumina and SiC using measured cooling rates shown in Fig. 6. The plots show that for alumina, the allowable stress of 300 MPa is exceeded. The predicted peak transient stress for SiC was < 20 MPa, rationalizing the successful performance observed. In (c), the model predictions for the TC location (solid lines) are shown compared with the experimental data (symbols) for the case of SiC sample holders (seen in Fig. 6).

short duration (5 min or less). Because of its high thermal conductivity, the peak temperature predicted for SiC was a lot less at 1400 K, with a thermal stress < 10 MPa, thus ensuring survival.

The alumina sample holder survived the vitiator-only condition but was found to have failed after the run with the combustion at ER = 0.5. The SiC sample holder survived all of the combustor segment cycles it was subjected to. The temperature measurements and visual observations are shown in Fig. 6. The experiment consisted of exposing two samples at a time, one closer to the center of the rig and the other closer to the wall, but both were outside the 0.5 in. boundary layer. The variation in gas temperatures resulted in a temperature difference between the two readings of about 50°C. The plots show the rapid cool down associated with combustor shut down.

Note that the total temperatures are much higher than the sample readings that were measured about 2.5 mm beneath the surface. The results from the thermostructural FEM modeling of the samples using the CFD results for the conditions of the test are shown in Fig. 7. In Fig. 7a, the predicted sample temperatures at the surface (peak) and at the measurement location (2.5 mm from surface) are shown for alumina and SiC, using the temperature-independent material properties shown in the plots. For alumina, the surface temperature is higher than the measured temperature but

still below the total temperature, as can be expected. The temperature at the TC location for SiC is very close to that in alumina, but the higher conductivity of SiC results in a lower surface (peak) temperature. In Fig. 7b, the steady-state and transient thermal stresses predicted by the model are shown for the cases of the alumina and SiC holders. The transient predictions were based on the cooling rates observed in the scramjet rig as shown in Fig. 6. It is observed that even though steady-state stresses were low, around 150 MPa (at the location shown in Fig. 5), the transients are predicted to be high enough to result in fracture for alumina. It is seen that for alumina the allowable stress of 300 MPa is exceeded. The predicted peak transient stress for SiC was <20 MPa, rationalizing the successful performance observed. In Fig. 7c, the model predictions (shown as lines) are compared with the experimentally measured temperature data (shown as symbols) using a plot that shows how the sample temperature varies with total temperature, which varied in discrete steps during the run as the vitiator and combustor ER settings were changed. The data are found to be in good agreement with the predictions, thus validating the model.

Figure 8 shows the results from the experimental run in which two LE specimens, one of SiC and another of 20% vol SiC–HfB_2 (UHTC), were subjected to hypersonic flow using the metallic sample holder. The measured temperatures are shown plotted along with the total temperature corresponding to the three combustor segment runs, with ER = 0.3, 0.4, and 0.45. Images captured from the video are shown for peak conditions and during cool down. Images of the samples before and after the run are included which show that the samples were intact during the entire run. The LE samples were removed from the holder with some difficulty, and these are shown in Fig. 9. The SiC sample broke during removal; it is possible that damage was introduced during the run that caused this failure. The UHTC sample was removed without any failure. There was no significant build up of oxidation products on the LE samples and no observable recession of the LE in both SiC and UHTC samples. Note that the bluntness observed at the tip of the SiC sample in Fig. 9 is due to an error in machining and was present before exposure. There were abrasion marks clearly visible where the dovetail holder and set screws contacted the LE sample. This indicated that there were significant vibrations and chatter from the acoustic conditions they were exposed to, and at least partly from variations in the flow. The SiC samples likely failed at this location during removal. The actual combustion gas composition varies with ER setting, and is shown in Fig. 10. It is seen that even at

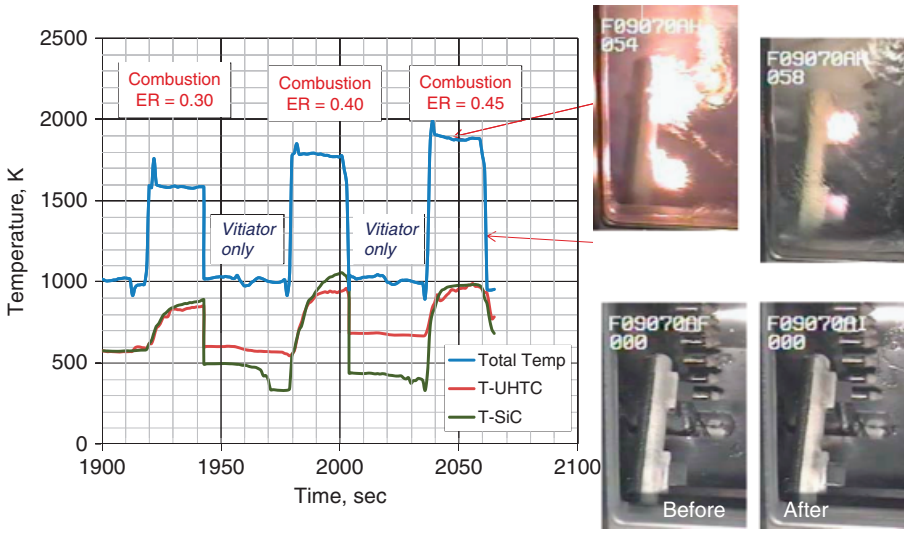

Fig. 8. A plot of total temperature versus time of exposure in the axisymmetric rig of leading edge (LE) samples of SiC and ultra high-temperature ceramics (UHTC) (20%SiC–HfB_2) using an internally cooled, thermal barrier-coated metallic sample holder. Thermocouple readings measured at the base of the 12.7 mm (0.5 in.)-long LE wedge samples are shown. The UHTC samples were close to the center of the rig, while the SiC sample was closer to the wall.

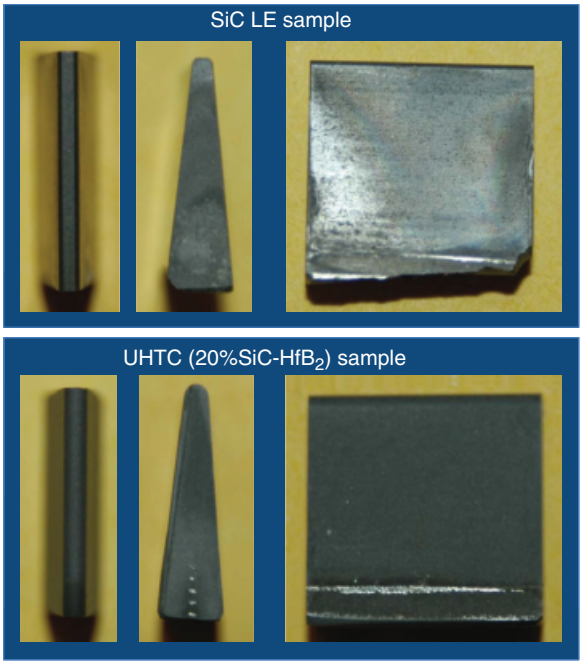

Fig. 9. The leading edge (LE) samples of SiC and ultra high-temperature ceramics (UHTC) after exposures in the axisymmetric rig subjected to equivalence ratios of 0.3, 0.4, and 0.45 as shown in Fig. 7. The samples survived the conditions without any noticeable degradation. The SiC sample broke during removal from the holder and it is possible that failure was initiated by the damage induced during the run. Evidence of mechanical vibrations can be seen from the abraded metallic material on the samples where the dovetail holder meets the sample, and where the set screw touches the sample, evident in the UHTC sample.

ER = 0.9 there is a significant amount of oxygen present; however, due to the short duration of the runs, oxidation of the samples was negligible.

Discussion

In this work, a new test procedure to subject materials directly to hypersonic flow was designed and has been demonstrated to be feasible. It remains to examine how well this method simulates the realistic conditions of hypersonic flight. We examine the conditions in the rig that are relevant to material survivability and compare them to those that exist during free flight; a good match should validate the methodology. Free-flight conditions are fully determined by Mach number and altitude; the conditions in the rig are fully determined

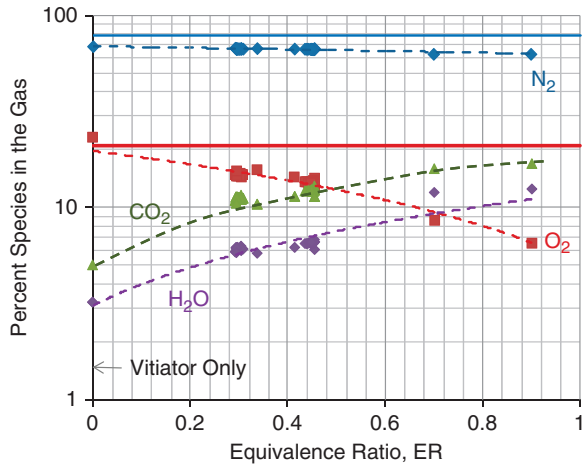

Fig. 10. The chemistry of the gases that the leading edge samples were exposed to varied with the level of combustion as determined by the equivalence ratio (ER) setting during the run, as shown by the dotted lines in the plot. The ER = 0 corresponds to vitiator-only condition. The solid blue and red lines correspond to the ambient composition for reference. In the rig, the oxygen decreases from near-atmospheric value in the vitiator-only state, to roughly half of it at a setting of ER = 0.6. There is a significant partial pressure of oxygen in the combusted gas mixture, and thus still a reasonable simulation of realistic conditions with regard to oxidation; however, there is a significant amount of H_2O and CO_2.

by total temperature, static pressure, and fluid velocity. Ideally, all important parameters for these two should match.

The parameters that characterize the aerothermal effects with respect to material survivability and thus a measure of simulation fidelity are (a) heat flux (fully catalytic), (b) total/stagnation temperature, (c) total/stagnation pressure, (d) dynamic pressure, (e) fluid velocity at the material surface (behind the shock wave), (f) fluid composition, (g) degree of dissociation of gaseous elements and catalytic recombination at material surface, and (h) mechanical loading from vibrations and shock. The first seven parameters can be measured or calculated. The last parameter is difficult to quantify; however, we believe the conditions in the scramjet rig are a good start for the simulation of real conditions in that vibrations and thermal shock were clearly present (evidenced by markings on the LE sample shown in Fig. 9).

Turning to the seven tractable parameters, fluid composition obtained from calibration of the rig is shown in Fig. 10. It is clear that nitrogen and oxygen

levels are not far from the ambient, but there is excess water and carbon dioxide. The other parameters can be calculated using equations given in the report by Ames Research Staff.[7] The aerothermal conditions as a function of altitude and Mach number were calculated using these equations. Equation 3 with $h_w = 0$ gives the cold wall heat flux. The other key equations used are reproduced below, with the same notation as in the report by Ames Research Staff.[7] The variation in ambient temperature and pressure with altitude is taken from the 1976 standard atmosphere, reproduced below for completeness[15]

$$T_1\,(K) = \begin{cases} 216.65 & 11\,\text{km} < h < 20\,\text{km} \\ 216.65 + (h - 20) & 20\,\text{km} < h < 32\,\text{km} \end{cases} \tag{6}$$

$$p_1\,(\text{kPa}) = \begin{cases} 22.632 e^{0.157688(h-11)} & 11\,\text{km} < h < 20\,\text{km} \\ 5.4749\left[1 - \frac{20-h}{216.65}\right]^{-34.163} & 20\,\text{km} < h < 32\,\text{km} \end{cases} \tag{7}$$

$$\rho(T,\,P)\,(\text{kg/m})^3 = \frac{p}{(0.2869\,T)};\; p\,(\text{kPa})\;T\,(\text{K}) \tag{8}$$

The total temperature given by Eq. (2) can be used to calculate the dynamic pressure, q, given by:

$$\frac{q}{p_{t1}} = \frac{\gamma}{\gamma - 1}\left(1 - \frac{T_1}{T_t}\right)\left(\frac{T_1}{T_t}\right)^{\frac{1}{1-\gamma}} \tag{9}$$

where p_{t1} is the total pressure ahead of the shock given as:

$$p_{t1} = p_1\left(1 + \frac{\gamma - 1}{2}M^2\right)^{\frac{\gamma}{\gamma-1}} \tag{10}$$

The equations below describe conditions ahead and behind the shock wave. The subscript 1 is used to describe parameters ahead of the shock wave (free stream) and 2 to describe parameters behind the shock wave.

$$\frac{p_2}{p_1} = \xi = \frac{2\gamma M_1^2 - (\gamma - 1)}{\gamma + 1} \tag{11}$$

$$M_2^2 = \frac{(\gamma - 1)\xi + (\gamma + 1)}{2\gamma\xi} \tag{12}$$

$$U_2 = M_2\sqrt{\gamma RT_2} \tag{13}$$

$$\frac{T_2}{T_1} = \frac{[2\gamma M_1^2 - (\gamma - 1)][(\gamma - 1)M_1^2 + 2]}{(\gamma + 1)^2 M_1^2} \tag{14}$$

In the above equations, subscripts 1 and 2 refer to conditions ahead and behind the shock wave, respectively. M_1 is the flight Mach number, M_2 the Mach number behind the shock, T_1 and T_2 the static temperature before and after the shock wave, respectively, T_t the total temperature, p_1 and p_2 the static pressure before and after the shock wave, respectively, and γ the ratio of specific heats of air taken as 1.4 in these calculations. Finally, while calculation of the actual dissociation extent under the shock wave is complex,[16] the upper limit on the degree of dissociation can be estimated using the rate constants given by Scala and Gilbert[17] as:

$$\log\frac{(P_O)^2}{P_{O_2}} = 6.8 - 26000/T;\; \log\frac{(P_N)^2}{P_{N_2}} = 7 - 50\,000/T \tag{15}$$

where P_O, P_N, and P_{O_2}, P_{N_2} refer to partial pressures in atmospheres of monatomic oxygen, nitrogen and molecular oxygen, nitrogen, respectively. The above equation, combined with total temperature (Eq. (2)) and static pressure behind shock, p_2 (Eq. (11)), gives an upper bound on the percent of oxygen and nitrogen dissociation behind the shock.

Figure 11 shows plots of the six parameters, total temperature, cold wall heat flux, dynamic pressure, fluid velocity behind the shock wave, static pressure behind the shock wave, and degree of dissociation of oxygen and nitrogen, for different flight Mach numbers calculated for an altitude of 28.1 km for a LE of radius 762 μm (30 mils), assuming a constant specific heat ratio of 1.4 for air. Note that the design window for actual hypersonic aircraft will be narrower, limited by allowable dynamic pressures. One method of evaluating the test is to examine how many of these parameters are simultaneously simulated within the test, and what is the effective Mach number the samples were subjected to. To implement this methodology, we choose to plot the heat flux, dynamic pressure, total pressure and fluid velocity in the rig against total temperature and compare the plots with what is predicted for free flight conditions at different altitudes and Mach numbers.

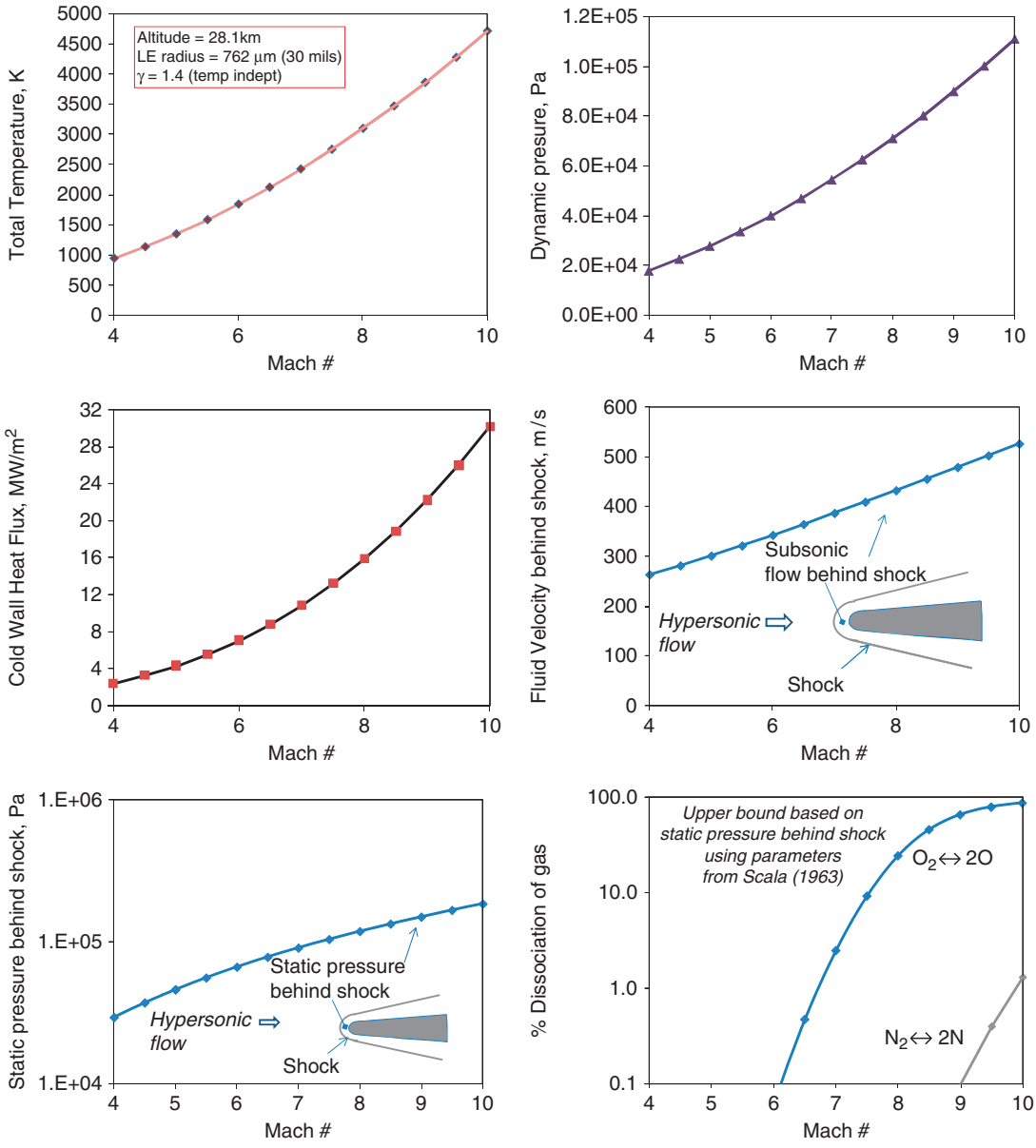

Fig. 11. The total temperature, dynamic pressure, fully catalytic heat flux, fluid velocity, and static pressure behind the shock wave, and the calculated degree of dissociation of gases are shown plotted as a function of flight Mach# at an altitude of 28.1 km and leading edge curvature radius of 762 μm (30 mils), assuming a constant value of 1.4 for γ, the ratio of specific heats of air.

The calibrations of the scramjet rig obtained using probes and detectors were used to determine the conditions during the actual runs used to expose the LE samples. The static pressure, total temperature and fluid velocity at the location of the samples were obtained and used to calculate heat flux, total temperature, fluid velocity at the material surface, dynamic pressure and total pressure. The total temperature is the primary reference parameter used to describe the flow conditions. Figure 12 shows the results of these calculations as data points, along with free flight conditions shown as lines for different altitudes and Mach numbers. It is seen that

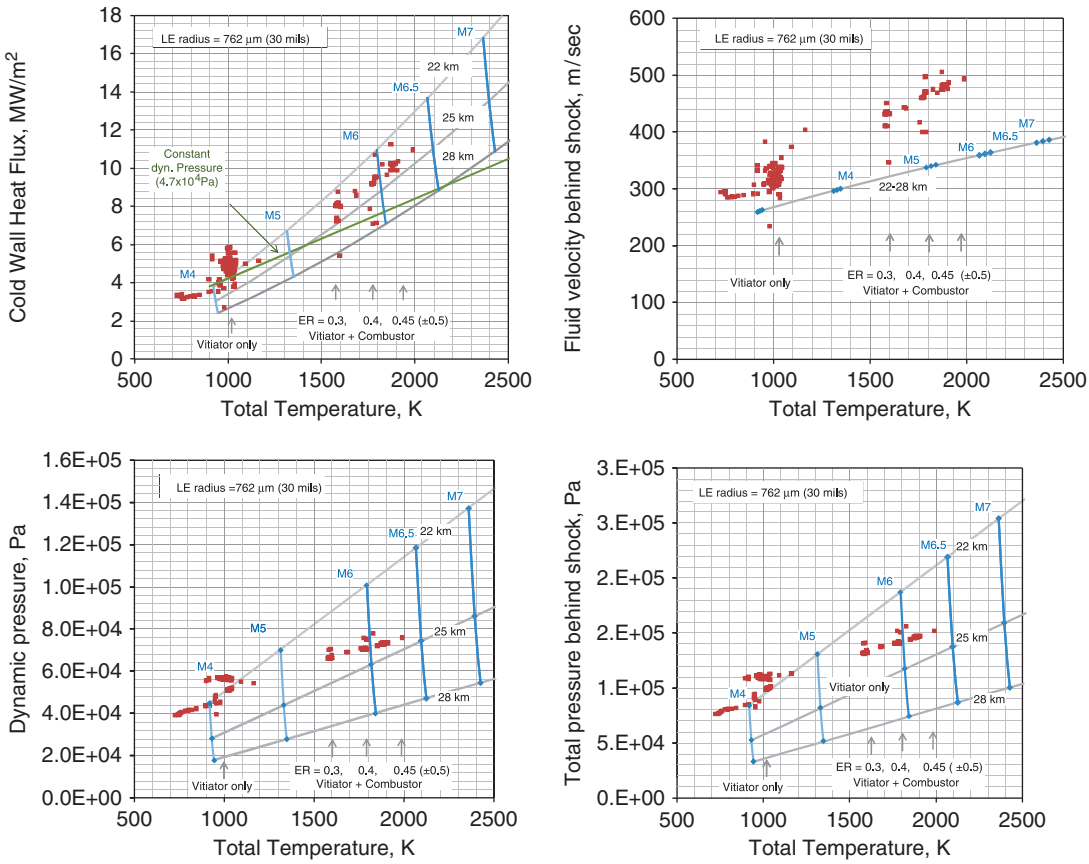

Fig. 12. Real flight conditions are specified in terms of Mach # and altitude. The conditions in the test rig are evaluated for the ability of the test to simulate the real flight conditions. Ideally, all parameters must be the same as in free-flight conditions, simultaneously. This is evaluated in these plots where the cold wall heat flux, fluid velocity behind shock, dynamic pressure, and total pressure behind the shock wave are plotted against total temperature and compared with values for flight conditions. The plot for heat flux also includes the constant dynamic pressure line. The conditions in the rig at equivalence ratio = 0.45 (the maximum value in each plot) is found to represent very closely the conditions during a Mach 6.5 flight at an altitude of 25 km.

the data points do not strictly follow the curves but are close. In particular near the maximum of the data set, where the samples were exposed to an ER = 0.45, the data points match well with the curve for 25 km and Mach 6.5. The fluid velocity at the material surface is higher than in real conditions but not by much. The degree of dissociation too was in agreement but not shown as it is seen to be unimportant (Fig. 11) for Mach numbers below 7.

It is important to note that there is a marked difference between the measured sample temperature and the known total temperature, as seen from Fig. 8. First, the finite heat transfer coefficient results in a lower surface temperature than the total temperature. Second, there is a steep gradient in heat flux from the tip of the LE, leading to a large drop in temperature at 12.7 mm (0.5 in.) from the LE, the location where the thermocouple was placed. This can be expected to result in a significantly lower temperature reading compared with that at the LE, as prior calculations have indicated.[5]

We conclude that the most severe condition in the scramjet rig to which the LE samples were exposed closely represents actual hypersonic flight conditions for a Mach number of 6.5 at an altitude of 25 km. We briefly summarize the limitations again. The key limitation is the presence of water and CO_2 in the gas atmosphere compared with the ambient, as seen from Fig. 10. Second, with respect to simulating the shear forces,

the fluid velocity behind the shock wave is larger than in real condition. The mechanical loading is expected to be similar to real conditions, but will vary with actual component design.

Summary

A method of evaluating materials for use in hypersonic flight components was developed, with a view to capture all essential aspects of real flight by directly exposing samples to hypersonic flow. The exposure was inside a prototype scramjet engine developed to study hypersonic combustion and propulsion efficiency. A combination of modeling and experimental trials was used to optimize the geometry and design of a sample holder that allowed the exposure of a sample to conditions that simulated free flight at speeds of up to Mach 7. The method was evaluated using aerothermal models and instrumented samples. It was shown that during a test in which both SiC and UHTC (20% vol $SiC–HfB_2$) LE samples survived, the conditions were very close to real flight conditions of Mach 6.5 at an altitude of 25 km. It is concluded that a method to expose and evaluate samples for LEs by directly exposing them to hypersonic flow that represents near flight conditions has been established.

Acknowledgments

We acknowledge technical support from Charles Smith, Richard Ryman, Jacob Diemer of ISSI, Dayton, OH and Steve Smith of AFRL/RZAS, WPAFB, OH, all of whom operated the scramjet rig with dedication and offered creative suggestions. One of the authors (TAP) acknowledges several useful discussions with Dr. T A Jackson (AFRL/RZ), Dr. D J Risha (AFRL/RZ), and Dr. R J Kerans (AFRL/RX), which provided the motivation for this work.

This work was supported in part by United States AFOSR.

References

1. T. A. Jackson, D. R. Eklund, and A. J. Fink, "High Speed Propulsion: Performance Advantage of Advanced Materials," *J. Mater. Sci.*, 39 5905–5913 (2004).
2. R. T. Voland, L. D. Huebner, and C. R. McClinton, "X-43A Hypersonic Vehicle Technology Development," *Acta Astronaut.*, 59 1818–1191 (2006).
3. S. Cook and U. Hueter, "NASA's Integrated Space Transportaion Plan—3rd Generation Reusable Launch Vehicle Technology Update," *Acta Astronaut.*, 53 719–728 (2003).
4. C. R. McClinton, V. L. Rausch, R. J. Shaw, U. Metha, and C. Naftel, "Hyper-X: Foundation for Future Hypersonic Launch Vehicles," *Acta Astronaut.*, 57 614–622 (2005).
5. R. J. Kerans, "Concurrent Material and Structural Design with Innovative Ceramic Composites," Final Report for DARPA/DSO [AFRL Technical Report: AFRL-ML-WP-TR-2006-4130], 2005.
6. M. M. Opeka, I. G. Talmy, and J. A. Zaykoski, "Oxidation-Based Materials Selection for 2000°C+ Hypersonic Aerosurfaces: Theoretical Considerations and Historical Experience," *J. Mater. Sci.*, 39 5887–5904 (2004).
7. Ames Research Staff, "Equations, Tables and Charts for Compressible Flow," National Advisory Committee for Aeronautics [Report 1135], 1953.
8. L. Lees, "On the Boundary Layer Equations in Hypersonic Flow and their Approximate Solutions," *J Aerosol. Sci.*, 20 [2] 143–145 (1953).
9. J. A. Fay and F. R. Riddell, "Theory of Stagnation Point Heat Transfer in Dissociated Air," *J Aerosol. Sci.*, 25 73–85 (1958).
10. M. Gruber, *et al.*, "Newly Developed Direct-Connect High-Enthalpy Supersonic Combustion Research Facility," *J Propul. Power*, 17 [6] 1296–1304 (2001).
11. T. Mathur, *et al.*, "Supersonic Combustion Experiments with a Cavity-Based Fuel Injector," *J Propul. Power*, 17 [6] 1305–1312 (2001).
12. J. T. C. Liu, *et al.*, "Near-Infrared Diode Laser Absorption Diagnostic for Temperature and Water Vapor in a Scramjet Combustor," *Appl. Opt.*, 44 [31] 6701–6711 (2005).
13. M. R. Gruber, R. A. Baurle, T. Mathur, and K. Y. Hsu, "Fundamental Studies of Cavity-Based Flameholder Concepts for Supersonic Combustors," *J Propul. Power*, 17 [1] 146–153 (2001).
14. E. V. Zoby, "Empirical Stagnation-Point heat-Transfer Relation in Several Gas Mixtures at High enthalpy Levels," NASA Tech Note, NASA TN D-4799, 1968.
15. NASA, "U.S. Standard Atmosphere," NOAA document ST 76-1562, 1976.
16. M. L. D. Silva, V. Guerra, and J. Loureiro, "State-Resolved Dissociation Rates for Extremely Nonequilibrium Atmospheric Entries," *J. Thermophys. Heat Transfer*, 21 [1] 40–49 (2007).
17. S. M. Scala and L. M. Gilbert, "Theory of Hypersonic Laminar Stagnation Region Heat Transfer in Dissociating Gase," NASA Tech Note NAS 7-100 Accession No. N71-70918, 1963.